Current Optics and Photonics
Vol. 4, No. 5, October 2020, pp. 441-445
ISSN: 2508-7266(Print) / ISSN: 2508-7274(Online)
DOI: https://doi.org/10.3807/COPP.2020.4.5.441

Design of a Fresnel Lens for a Solar End-pumped Solid-state Laser

Mingyu Ou[1], Pian Hu[1], Lanling Lan[1], Yan Liu[1,2]*, Jun Zhou[3], and Xiaotao Shi[2]**

[1]*College of Science, China Three Gorges University, Yichang 443002, China*
[2]*Hubei International Science and Technology Cooperation Base of Fish Passage, China Three Gorges University, Yichang 443002, China*
[3]*Shanghai Institute of Optics and Fine Mechanics, Chinese Academy of Sciences, Shanghai 201800, China*

(Received July 21, 2020 : revised September 5, 2020 : accepted September 7, 2020)

A novel design for a Fresnel lens for a solar end-pumped laser is demonstrated in this paper. The new hybrid Fresnel lens includes two parts, inner and outer. The inner part is a twice-total-internal-reflection and vertical-transmission lens. The outer part is a once-total-reflection and vertical-transmission lens. The radius of the Fresnel lens is 600 mm, and its focal length is 750 mm. The concentrating performance of the Fresnel lens is examined using TracePro. The results show that the concentration efficiency has been greatly improved. The total concentration efficiency of the hybrid Fresnel lens reaches 73.2% when the radius of the laser rod is 3 mm. This design can simplify the concentration system of a solar end-pumped solid-state laser.

Keywords : Solar pumped laser, Fresnel lens, Concentration efficiency
OCIS codes : (140.3580) Lasers, solid-state; (140.5560) Pumping; (350.6050) Solar energy

I. INTRODUCTION

The solar pumped laser is an important way of utilizing solar energy. A solar pumped laser offers attractive prospects for many applications in the future, including space laser communication, space energy transmission, and magnesium resource recycling [1-3]. The solar laser has attracted more and more attention [4, 5]. The solar concentrating system is very important for a solar pumped laser, and can affect the total conversation efficiency and laser output power directly [6-8].

Fresnel lenses have been used as the primary concentrator of a solar pumped laser because they can offer high concentrating efficiency, along with minimal weight and low cost. In fact, Fresnel lenses have been widely used in the fields of projection display, illumination, and solar-energy utilization [9-11]. The conventional Fresnel lens has a surface consisting of a concentric series of simple lens sections. The material of the Fresnel lens for many solar pumped laser systems is poly(methyl methacrylate) (PMMA). This material is a typical optical plastic that is transparent to most of the wavelengths in the solar spectrum.

Abdel-Hadi reported a laser concentration system including a Fresnel lens and CPC (composite parabolic concentrator) [12]; the area of the Fresnel lens was 60 cm × 60 cm and the focal length 0.75 m. Fang demonstrated a three-stage concentrator system [13], the first stage being a Fresnel lens (0.98 m × 1.2 m, f = 1.3 m). Liang reported a three-stage multi-Fresnel lens that was adopted for a side-pumping solar laser [14]; each part was composed of 32 pairs of narrow plane mirrors and Fresnel lenses. The pumping approach of a scalable TEM_{00} solar laser was also three-stage system in [15], in which the first-stage had a four-pair Fresnel lens-folding mirror collector. Each Fresnel lens diameter was 1.13 m and the focal length 2 m. Yang used a 1.03 m^2 Fresnel lens as the primary concentrator for a 28 W solar laser [16].

It is difficult to use a conventional Fresnel lens with large size directly for a solar end-pumped laser, because dispersion and sunlight of divergent angle cause a larger

*Corresponding author: liuyan703@163.com, ORCID 0000-0003-2806-9264
**Corresponding author: 57273002@qq.com, ORCID 0000-0002-9419-308X
Color versions of one or more of the figures in this paper are available online.

focal-spot size. To enhance concentration efficiency, usually a second concentrator needs to be utilized.

A Fresnel lens $1.4 \times 1.05\ m^2$ in size and with focal length of 1.2 m was used as a concentrator for a solar pumped laser. The measured full width at half maximum (FWHM) of the focal point was about 11 mm, and a cylindrical cavity was used to enhance the coupling to the laser media [17]. Another Fresnel lens ($2 \times 2\ m^2$, $f = 2000$ mm) was also adopted as a concentrator for a solar pumped laser with the diameter of the focal point limited to 20 mm. A conical cavity was used to enhance the solar-power absorption by the laser media [18]. A laser output of about 80 W was achieved with a combination of Fresnel lenses 4 m^2 in area and 2 m in focal length. The FWHM of the Fresnel lens's focal point was 20.4 mm, and a pumping cavity was used as a secondary power concentrator [19]. A Fresnel lens 0.9 m in diameter acted as a primary concentrator, with a measured FWHM of the focal point of about 12 mm, while a dielectric totally internally reflecting device was employed as a secondary concentrator [20]. A 1-m-diameter Fresnel lens also acted as concentrator, with focal length 1.3 m and FWHM of the focal point 13 mm. A large aspheric lens and a 2D-CPC were used to further compress the concentrated solar radiation [21]. Also, four 800 mm × 800 mm Fresnel lenses were used as a primary concentrator, the FWHM diameter of the focal spot being 12 mm, while aspherical lenses and a fused-silica sphere were used for further concentration [22].

Compared to the side-pumped laser, the end-pumped laser not only has high pump efficiency, but also can easily achieve laser output with good beam quality [23]. If the concentrator for a solar end-pumped laser were a single Fresnel lens without a secondary optical element, the structure would be simpler and adjustment would be more convenient. Thus it is necessary to design a novel Fresnel lens to meet this need.

II. FRESNEL LENS DESIGN BASED ON ONCE TOTAL INTERNAL REFLECTION

Figure 1 shows the schematic diagram of a Fresnel lens based on once total internal reflection (OTIR). The prism of the Fresnel lens is composed of two parallel surfaces and one surface that is perpendicular to the emergent light. In this figure, b is the groove pitch, d is the height of the prism, α is the dip angle of two parallel surfaces, and θ is the rim angle. The focal length is F. The distance between the central incident-light ray of the prism and the optical axis is D. H is the height of the current prism, and t is the thickness of the Fresnel lens (3 mm). The groove pitch is 0.33 mm.

The relationship of the parameters is as follows:

$$\alpha = (\pi - \theta)/2, \quad (1)$$

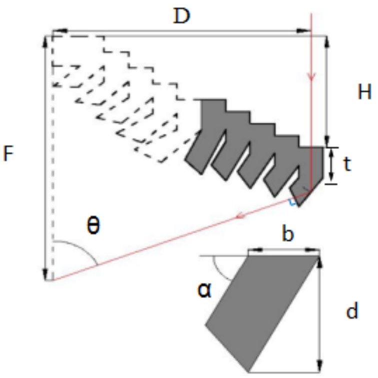

FIG. 1. Schematic of a Fresnel lens based on OTIR.

$$\theta = \arctan\left[D/(F - H - \frac{b\tan(\alpha)}{2} - t) \right]. \quad (2)$$

The angle α decreases with increasing D in this design, when the focal length is maintained. It causes the two adjacent prisms to overlap, and part of the light will be blocked. To overcome this problem, each prism increases by a step in height relative to the upper prism, and the whole structure is a staircase. According to Eqs. (1) and (2), the structure of this kind Fresnel lens can be given.

However, d increases rapidly when D decreases. This leads to the design becoming inappropriate. This design is suitable for the outer part of the Fresnel lens, where the radius is 300 to 600 mm. To compensate for the defects of this design, we propose another design for the inner part as follows.

III. FRESNEL LENS DESIGN BASED ON TWICE TOTAL INTERNAL REFLECTION

Figure 2 shows the Fresnel lens design based on twice total internal reflection (TTIR). The prism consists of surfaces of a fixed tilt angle β, a gradient angle α, and a plane perpendicular to the emergent light. Angle β was set to $\pi/4$. The thickness of the Fresnel lens t is set to 3 mm.

The height of each prism also increases relative to the upper prism, for the same reason as in the outer part of the Fresnel lens. The parameters' relationship is as follows:

$$2\alpha - \theta - 2\beta = 0, \quad (3)$$

$$\theta = \arctan\left(\frac{M_1}{M_2} \right), \quad (4)$$

$$M_1 = D - \left(\frac{b\tan(\alpha)}{2\tan(\beta)} + \frac{b}{2} - \frac{b}{2} \bullet \frac{\tan(\alpha) + \tan(\beta) - \tan^2(\alpha)\tan(\beta) - \tan^3(\alpha)}{2\tan(\alpha)\tan^2(\beta) + \tan(\beta) - \tan^2(\alpha)\tan(\beta)} \right), \quad (5)$$

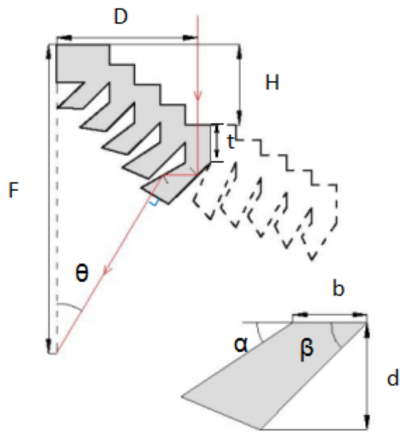

FIG. 2. Schematic of a Fresnel lens based on TTIR.

$$M_2 = F - H - t - \frac{b}{2}\tan(\alpha) - (D - M_1)\tan\left(2\alpha - \frac{\pi}{2}\right). \quad (6)$$

According to Eqs. (3)-(6), the structure of this kind Fresnel lens can be given. This method is used to design the inner part of the Fresnel lens.

IV. SIMULATION AND ANALYSIS

The structure of the hybrid Fresnel lens is shown in Fig. 3. This hybrid Fresnel lens includes two parts, the inner part and the outer part. The radius of the inner part is 300 mm, and the radius of the outer part is from 300 to 600 mm. The inner part is a twice-total-internal-reflection and vertical-transmission lens. The outer part is a once-total-reflection and vertical-transmission lens. The material of the Fresnel lens is PMMA. The concentrating performance of the Fresnel lens was studied using the TracePro optical software.

To optimize the design, the relationship between concentration efficiency and the Fresnel lens's focal length is

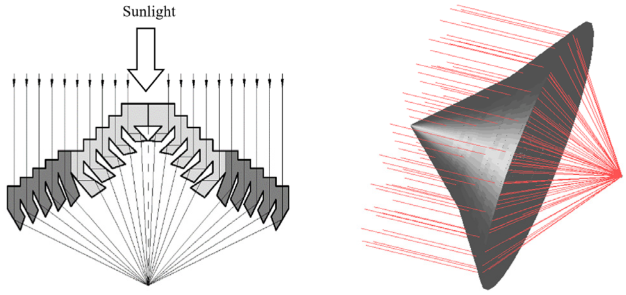

FIG. 3. Schematic diagram of the hybrid Fresnel lens.

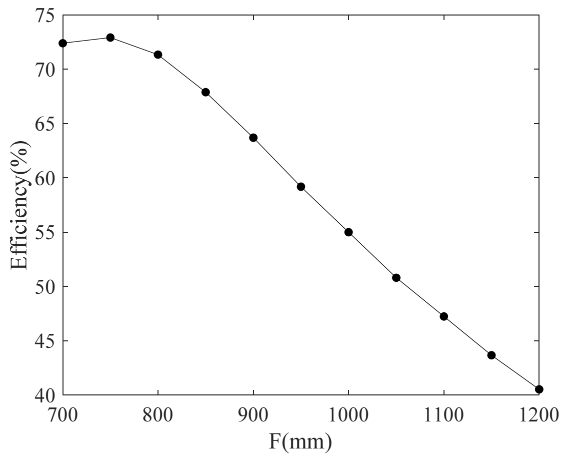

FIG. 4. Relationship between efficiency and focal length.

demonstrated in Fig. 4, when the receiver radius is 3 mm. Figure 4 shows that the concentration efficiency changes when the focal length varies from 700 to 1200 mm. The maximum efficiency of 73.2% is reached when the focal length is 750 mm, so the hybrid Fresnel lens's focal length is set to that value.

Figure 5 shows the irradiation of the hybrid Fresnel lens's focus spot. The wavelength of incident light also ranges from 374 to 1642 nm in the simulation.

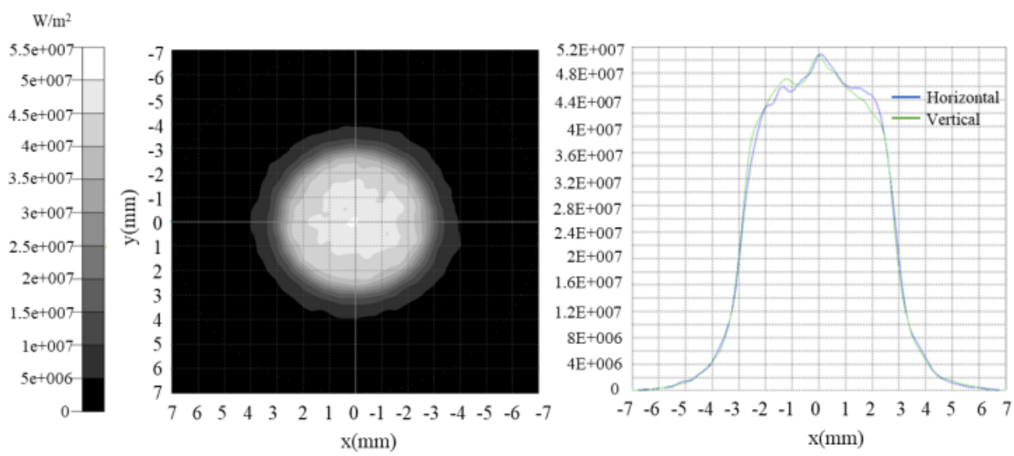

FIG. 5. Irradiation of the hybrid Fresnel lens's focus spot.

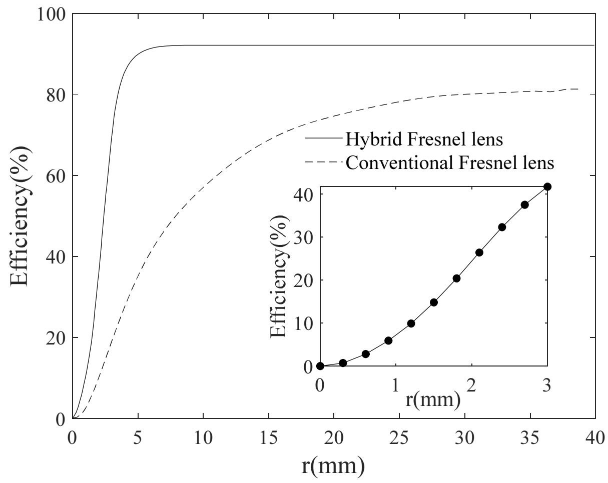

FIG. 6. Relationship between concentration efficiency of the system and receiver radius.

Figure 6 shows that the efficiency changes as the receiver radius ranges from 0 to 40 mm. The curvature of the hybrid Fresnel lens increases more sharply than that of the conventional Fresnel lenses mentioned earlier in refs. 24 and 25. Focal length, groove pitch, thickness, and diameter of the conventional Fresnel lens that is compared are respectively 750 mm, 0.33 mm, 3 mm, and 1200 mm [24, 25]. The concentration efficiencies of the hybrid and conventional Fresnel lenses are 37.3% and 9.7% respectively when the receiver radius is 2 mm, and are 73.2% and 19.1% respectively when the receiver radius is 3 mm. This means that collection of the sun's energy by the hybrid Fresnel lens is 3.7 times as great as by the conventional Fresnel lens, if the radius of laser rod is 3 mm and end pumping is adopted. The maximum efficiency of the hybrid Fresnel lens is 92.1%, when r is 6.5 mm; that of the conventional Fresnel lens is 80.8%, when r is 37.5 mm.

The inset of Fig. 6 demostrates that the total concentrator efficiency is 40.2% when a CPC is at the focal plane of the Fresnel lens. After optimizing the position of the CPC, the maximum concentration efficiency can reach 50.4% [24]. Even when a dielectric-filled CPC is used to improve the efficiency, the total concentrating efficiency of the secondary concentrating system is only 64.1% [26].

The FWHM of the hybrid Fresnel lens's focal point is 5.6 mm. This result also has advantage over that for the Fresnel lenses in refs. 17-22.

V. CONCLUSION

In this paper, a novel hybrid Fresnel lens for a solar end-pumped solid-state laser was reported. The new hybrid Fresnel lens includes two parts, the inner part and the outer part. The inner part is a twice-total-internal-reflection and vertical-transmission lens. The outer part is a oncetotal-reflection and vertical-transmission lens. The focal length of the Fresnel lens is 750 mm, the radius of the inner part is 300 mm, and the radius of the outer part is from 300 to 600 mm. The concentration efficiency of this hybrid Fresnel lens is 73.2%, when the receiver radius is 3 mm. This means that collection of the sun's energy by the hybrid Fresnel lens is improved greatly, so a secondary concentrator becomes unnecessary, and the concentrator system can be simpler. This kind of Fresnel lens can also be used in other fields, such as concentrated photovoltaics and solar thermal utilization.

ACKNOWLEDGMENT

This work is supported by the Shanghai Key Laboratory of All Solid-State Laser and Applied Techniques Foundation Program (2013ADL02), and the Nature Science Foundation of Hubei Province (2014CFB671).

REFERENCES

1. T. Saiki, S. Taniguchi, K. Nakamura, and Y. Iida, "Development of solar-pumped lasers and its application," Electr. Eng. Jpn. **199**, 3-9 (2017).
2. S. Mizuno, H. Ito, K. Hasegawa, T. Suzuki, and Y. Ohishi, "Laser emission from a solar-pumped fiber," Opt. Express **20**, 5891-5895 (2012).
3. Z. Guan, C. M. Zhao, S. H. Yang, J. Y. Ke, and H. Y. Zhang, "Demonstration of a free-space optical communication system using a solar-pumped laser as signal transmitter," Laser Phys. Lett. **14**, 055804 (2017).
4. M. Endo, J. F. Bisson, and T. Masuda, "Monte carlo simulation of a transversely excited solar-pumped fiber laser," Jpn. J. Appl. Phys. **58**, 112006 (2019).
5. T. Kato, H. Ito, K. Hasegawa, T. Ichikawa, A. Ikesue, S. Mizuno, Y. Takeda, A. Ichiki, and T. Motohiro, "Effect of Cr content on the output of a solar-pumped laser employing a Cr-doped Nd:YAG ceramic laser medium operating in sunlight," Jpn. J. Appl. Phys. **58**, 062007 (2019).
6. W. Fan, Y. Liu, P. Guo, R. Deng, N. Li, F. Ding, Y. Li, J. Zhou, and S. Xie, "Design of concentrating system for solar side-pumped slab laser," Curr. Opt. Photon. **4**, 50-56 (2020).
7. M. Lando, J. Kagan, B. Linyekin, and V. Dobrusin, "A solar pumped Nd:YAG laser in high collection efficiency regime," Opt. Commun. **222**, 371-381 (2003).
8. Z. C. Shen, Y. Lu, and J. Y. Lu, "Fresnel lens solar concentrator design and spectral distribution on focus surface," Opt. Rev. **18**, 398 (2011).
9. W. T. Xie, Y. J. Dai, R. Z. Wang, and K. Sumathy, "Concentrated solar energy applications using Fresnel lensed: A review," Renew. Sustain. Energy Rev. **15**, 2588-2606 (2011).
10. X. Gao, X. Sang, X. Yu, X. Cao, Z. Chen, B. Yan, J. Yuan, K. Wang, C. Yu, W. Dou, and L. Xiao, "High brightness three-dimensional light field display based on the aspheric substrate Fresnel-lens-array with eccentric pupils," Opt. Commun. **361**, 47-54 (2016).

11. N. H. Vu, T. T. Pham, and S. Shin, "LED uniform illumination using double linear Fresnel lensed for energy saving," Energies **10**, 2091 (2017).
12. Y. A. Abdel-Hadi, "Simulation model of a new solar pumped laser of Fresnel lens in Helwan of Egypt," NRIAG J. Astron. Geophys. **1**, 195-198 (2012).
13. D. Fang, X. H. Wang, F. Wang, and S. N. Liu, "Solar pumped Nd:YAG laser," Optik **124**, 3367-3370 (2013).
14. D. Liang and J. Almeida, "Multi-Fresnel lenses pumping approach for improving high-power Nd:YAG solar laser beam quality," Appl. Opt. **52**, 5123-5132 (2013).
15. D. Liang, J. Almeida, and C. R. Vistas, "Scalable pumping approach for extracting the maximum TEM_{00} solar laser power," Appl. Opt. **53**, 7129-7137 (2014).
16. S. H. Yang, P. Xu, C. M. Zhao, Z. Guan, H. X. Wang, Y. C. Zhang, H. Y. Zhang, and T. He, "28 W solar-pumped laser with a grooved Nd:YAG rod," in Advanced Solid State Lasers (Shanghai, China, 2014), ATu2A.45.
17. T. Yabe, T. Ohkubo, S. Uchida, K. Yoshida, M. Nakatsuka, T. Funatsu, A. Mabuti, A. Oyama, K. Nakagawa, T. Oishi, K. Daito, B. Behgol, Y. Nakayama, M. Yoshida, S. Motokoshi, Y. Sato, and C. Baasandash, "High-efficiency and economical solar-energy-pumped laser with Fresnel lens and chromium codoped laser medium," Appl. Phys. Lett. **90**, 261120 (2007).
18. T. Yabe, B. Bagheri, T. Ohkubo, S. Uchida, M. Yoshida, T. Funatsu, T. Oishi, K. Daito, M. Ishioka, N.Yasunaga, Y. Sato, C. Baasandash, Y. Okamoto, and K. Yanagitani, "100 W-class solar pumped laser for sustainable magnesium-hydrogen energy cycle," J. Appl. Phys. **104**, 083104 (2008).
19. T. Ohkubo, T. Yabe, K. Yoshida, S. Uchida, T. Funatsu, B. Bagheri, T. Oishi, K. Daito, M. Ishioka, Y. Nakayama, N. Yasunaga, K. Kido, Y. Sato, C. Baasandash, K. Kato, T. Yanagitani, and Y. Okamoto, "Solar-pumped 80 W laser irradiated by a Fresnel lens," Opt. Lett. **34**, 175-177 (2009).
20. D. Liang and J. Almeida, "Highly efficient solar-pumped Nd:YAG laser," Opt. Express **19**, 26399-26405 (2011).
21. D. Liang and J. Almeida, "Solar-pumped TEM_{00} mode Nd:YAG laser," Opt. Express **21**, 25107-25112 (2013).
22. B. Galinhas and D. Liang, "End-side-pumped Nd:YAG solar laser with four Fresnel lenses," Proc. SPIE. **8785**, 87850G (2013).
23. T. Y. Fan and A. Sanchez, "Pump source requirements for end-pumped lasers," IEEE J. Quantum Electron. **26**, 311-316 (1990).
24. P. Hu, Y. Liu, S. G. Zeng, X. R. Chang, J. Zhou, S. Q. Feng, and X. T. Shi, "The influence of compound parabolic concentrator parameters on the solar laser condensation efficiency," Laser J. **38**, 8-11 (2017).
25. P. P. Luo, C. Liu, P. Xu, C. M. Zhao, S. H. Yang, and Y. L. Qian, "Solar pumped Nd:YAG laser with Fresnel lens," Chin. J. Lasers. **38**, 1002002-1 (2011).
26. W. T. Fan, R. C. Wang, Y. S. Li, Y. Liu, Q. Wang, J. Zhou, F. K. Ding, M. Y. Ou, and X. T. Shi, " The influence of solid dielectric CPC on concentration effect of solar laser," Laser J. **12**, 1-5 (2019).